

ScarletNAS: Bridging the Gap Between Scalability and Fairness in Neural Architecture Search

Xiangxiang Chu¹, Bo Zhang¹, Jixiang Li¹, Qingyuan Li², Ruijun Xu¹

¹Xiaomi AI Lab, ²Xiaomi IoT

{chuxiangxiang, zhangbo11, lijixiang, liqingyuan, xuruijun}@xiaomi.com

Abstract

One-shot neural architecture search features fast training of a supernet in a single run. A pivotal issue for this weight-sharing approach is the lacking of scalability. A simple adjustment with identity block renders a scalable supernet but it arouses unstable training, which makes the subsequent model ranking unreliable. In this paper, we introduce linearly equivalent transformation on identity blocks to soothe training perturbation, providing with the proof that such a transformed model is identical with the original one as per representational power. Our overall method is hereby named as SCARLET (SCALable supeRnet with Linearly Equivalent Transformation). We show through experiments that linearly equivalent transformations can indeed harmonize the supernet training. With an EfficientNet-like search space and a multi-objective reinforced evolutionary backend, it generates a series of competitive models: SCARLET-A achieves 76.9% top-1 accuracy on ImageNet which outperforms EfficientNet-B0 by a large margin; the shallower SCARLET-B exemplifies the proposed scalability which attains the same accuracy 76.3% as EfficientNet-B0 with much fewer FLOPs. Moreover, our manually scaled SCARLET-A2 hits 79.5%, SCARLET-A4 82.3%, which are on par with EfficientNet-B2 and EfficientNet-B4 respectively. The models and evaluation code will be released online.¹

Introduction

Neural architecture search has been recently dominated by one-shot methods (Brock et al. 2018; Bender et al. 2018; Stamoulis et al. 2019; Guo et al. 2019; Cai, Zhu, and Han 2019). Fundamentally, a supernet which incorporates the whole search space enjoys fast convergence through weight sharing. Evaluating the performance of models by picking a single path from the supernet then becomes handy. According to FairNAS (Chu et al. 2019), fair training of supernet shows a remarkable improvement in model ranking. However, previous supernets are limited by their fixed depth. By contrast, as pure reinforcement or evolutionary approaches train each model independently for evaluation, shallower models can also stand out if they exhibit good performance. This step is very beneficial as it achieves automatic architectural compression. To enable the similar property for the

family of one-shot methods, we install identity choice blocks for network downscaling, which are accompanied with *linearly equivalent transformation* as a relay for inter-block information.

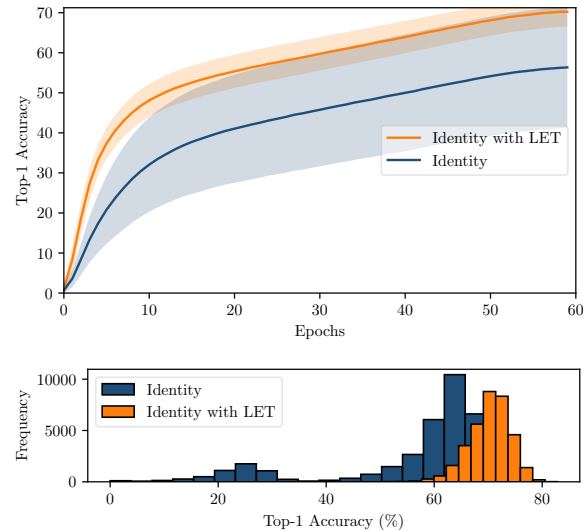


Figure 1: Training process of scalable supernets with and without linearly equivalent transformation (LET). **Top:** The accuracy of supernet with LET has much smaller standard variance. **Bottom:** Histogram of training accuracies of sampled one-shot models³ within last epoch.

To summarize, our main contributions are threefold.

- We introduce *Linearly Equivalent Transformation* (LET) for identity blocks to enable a supernet to incorporate models of variable depths, while retaining training stability and accuracy. We show that identity blocks alone would fail as it disturbs supernet training, see Figure 1.
- We prove the equivalence of models under our naive adjustment with linearly equivalent transformation. This is critical to maintain the same representation power for stand-alone models when LET is removed.

¹<https://github.com/xiaomi-automl/SCARLET-NAS>

³A one-shot model is a path with weights loaded from supernet.

- We generate networks of overwhelming performance in **12 GPU days**, compared to their counterparts especially EfficientNet (Tan and Le 2019). SCARLET-A claims a new state of the art **76.9%** top-1 accuracy on ImageNet at the level of 400M multiply-adds. SCARLET-C also reaches competitive 75.6% with much decreased multiply-adds. More importantly, the closest model to EfficientNet-B0, SCARLET-B, which is a shallow version from our search space, distinguishes itself with 76.3%. Besides, our manually scaled models SCARLET-A2, A4 are also comparable to EfficientNet-B2, B4 accordingly.

Review of the Depth-variable Supernet Training

It has been unheeded about the training of scalable supernets, at least not carefully dealt with. Generally, mainstream one-shot approaches suffer from unstable training (Bender et al. 2018). This problem deteriorates when scalability is considered. Zero operations are added to skip blocks in (Cai, Zhu, and Han 2019) to have flexibility in width and depth, however, its training details are not thoroughly discussed. (Guo et al. 2019) also adopts the same search space design to draw a fair comparison. The intermediate process is also not reported, we can not decide how much difference do skip connections make.

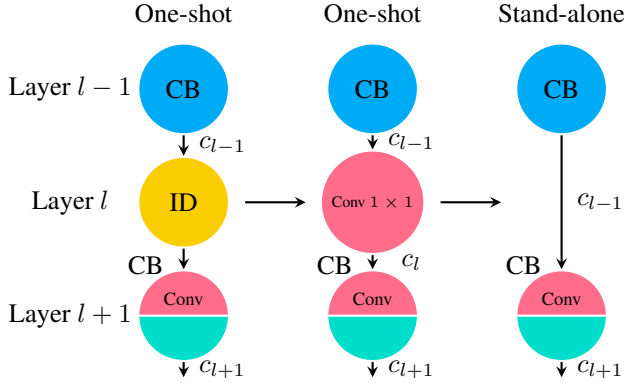


Figure 2: Identity with linearly equivalent transformation. CB: Choice Block. ID: Identity. Note c_l means the output channel size of layer l . Note the Conv operation in layer $l+1$ can also be an FC.

We are motivated by FairNAS which displays interesting feature maps after first choice blocks. It attests that all choice blocks learn similar knowledge, even at correspondent channels. This is an important incentive for us to investigate further whether a fair training of scalable supernet is possible. We notice that simply introducing identity blocks breaks training stability. As other blocks are all learning units, identity blocks don't learn any information, which destroys balance during training. Hence, we could accommodate this defect by injecting a learning unit. Here we remedy the issue with 1×1 convolution without non-linear activations. It is named as linearly equivalent transformation (LET), see Figure 2. Be aware the difference that layer $l+1$ in stand-alone

models have $c_{l-1} * c_{l+1}$ parameters, while its one-shot counterparts have $c_l * c_{l+1}$.

Stabilizing Training by Linearly Equivalent Transformation

A critical requirement for transformation is equivalence. Thus, the transformed model behaves exactly as the original entity. To proceed, we first define the equivalence.

Definition 1. Given a valid space X , a function f is equivalent to g on X if and only if $f(x) = g(x)$ for $x \in X$, where x , $f(x)$ and $g(x)$ are tensors of any shape.

Definition 2. The equivalence of two neural networks: for models A and B with weights θ_A and θ_B , $A = B$ if and only if f_A and f_B are equivalent.

The 2D convolution and fully-connected layer are two of the most widely used operations in deep neural networks. For the image classification task, a mini-batch b of $h \times w$ images with c channels can be denoted by $I_0(b, h, w, c)$. Let A be a deep neural network with L layers and I_l be the feature maps of the l -th layer. For simplicity, we omit the batch dimension. Say F_l is the operation of layer l , we have,

$$I_l = F_l(I_{l-1}) \quad (1)$$

In general, there are mainly fully-connected operations and 2D convolutions, so the shape of I_l can be either (c_l) or (h_l, w_l, c_l) . We denote a 2D convolution as $Conv(c_{in}, c_{out}, kernel, stride)$. For convenience, we examine only square kernels with $stride = 1$ and neglect dilation rates. Other setups can be easily proven in the same manner. Primarily, we discuss these two scenarios:

- I_{l-1} and I_l have shape (c_{l-1}) and (c_l) respectively. F_l is a linear operation without activation and the first operation of F_{l+1} is a linear (fully-connected) $FC_{(c_l, m)}$,
- I_{l-1} and I_l each have shape $(h_{l-1}, w_{l-1}, c_{l-1})$ and (h_l, w_l, c_l) . F_l is a 2D convolution $Conv_{(c_{l-1}, c_l, 1, 1)}$ without activation or bias. The first operation of F_{l+1} is 2D convolution $Conv_{(c_l, m, k, 1)}$.

Note that the choice block in a layer can either be a simple or a complex block and we only require that the beginning part of it is a 2D convolution or an FC. This requirement is weak enough to cover most neural networks.

Lemma 1. For the first scenario, we replace F_l and $FC_{(c_l, m)}$ with an identity operation and another linear $FC_{(c_{l-1}, m)}$ to construct B from A , then we can ensure $A = B$.

Proof. First, we copy B 's weights from A except for F_l and $FC_{(c_l, m)}$. We can make $A = B$ if we can let $FC_{(c_{l-1}, m)}$ be equivalent to the above two successive operations. For any $x \in \mathbf{R}^{c_{l-1}}$, let $W_{c_{l-1} \times c_l}$ and $W_{c_l \times m}$ denote the weight matrices of $FC_{(c_{l-1}, c_l)}$ and $FC_{(c_l, m)}$. Let $W_{c_{l-1} \times m}$ be the weight matrix of $FC_{(c_{l-1}, m)}$.

Second, we can calibrate

$$W_{c_{l-1} \times m} = W_{c_{l-1} \times c_l} W_{c_l \times m}.$$

We can make $A = B$ by combining them both. \square

Lemma 2. For the second scenario, we substitute F_l and $Conv_{(c_l, m, k, 1)}$ with an identity operation and another 2D convolution $Conv_{(c_{l-1}, m, k, 1)}$ to construct B from A , then we can ensure $A = B$.

Proof. First, we copy B 's weights from A except for the F_l and $Conv_{(c_l, m, k, 1)}$. The only thing to prove is that we can replace F_l and $Conv_{(c_l, m, k, 1)}$ with $Conv_{(c_{l-1}, m, k, 1)}$ equivalently.

Second, We prove that any $x \in \mathbf{R}^{h, w, c_{l-1}}$, the above declaration holds. Let $W_{c_{l-1}, c_l, 1, 1}^1$ and $W_{c_l, m, k, k}^2$ be the weight tensor of F_l and $Conv_{(c_l, m, k, 1)}$. Let $W_{c_{l-1}, m, k, k}^3$ be the weight tensor of $Conv_{(c_{l-1}, m, k, 1)}$. Let w be one element of the tensor.

$$\begin{aligned} y &= F_l(x) \\ z &= Conv_{(c_l, m, k, 1)}(y) \\ y(i, j, c) &= \sum_{p=1}^{c_{l-1}} w_{p, c, 1, 1}^1 x(i, j, p) \end{aligned}$$

Also,

$$\begin{aligned} z(i, j, c) &= \sum_{q=1}^k \sum_{p=1}^{c_l} w_{p, c, q, q}^2 y(i+q, j+q, p) \\ &= \sum_{q=1}^k \sum_{p=1}^{c_l} w_{p, c, q, q}^2 \left(\sum_{u=1}^{c_{l-1}} w_{u, p, 1, 1}^1 x(i+q, j+q, u) \right) \\ &= \sum_{q=1}^k \sum_{p=1}^{c_l} \sum_{u=1}^{c_{l-1}} w_{p, c, q, q}^2 w_{u, p, 1, 1}^1 x(i+q, j+q, u) \\ &= \sum_{q=1}^k \sum_{u=1}^{c_{l-1}} \sum_{p=1}^{c_l} w_{p, c, q, q}^2 w_{u, p, 1, 1}^1 x(i+q, j+q, u) \\ &= \sum_{q=1}^k \sum_{u=1}^{c_{l-1}} w_{u, c, q, q}^3 x(i+q, j+q, u) \end{aligned}$$

We can make $A = B$ by setting

$$w_{u, c, q, q}^3 = \sum_{p=1}^{c_l} w_{p, c, q, q}^2 w_{u, p, 1, 1}^1.$$

Thus it is proved. \square

Since we don't search the number of channels, we replace the choice identity with 1×1 convolution without bias or activation for convolution networks and FC layer without activation when the identity is needed between FC layers. This procedure is illustrated in Figure 2. The left-most architecture is the original and commonly used version. The middle one is its equivalent version and the right-most version is the architecture for stand-alone training. Attention should be paid for training stand-alone models. The number of feature maps usually increases with depth. For instance, in Figure 2, $c_{l+1} \geq c_l \geq c_{l-1}$, we should adjust the input channel number to make convolution works.

Searching with Multi-Objective NAS Pipeline

Upon a ready-to-use scalable supernet, we take advantage of a multi-objective approach to serve as our search pipeline as (Deb et al. 2002; Lu et al. 2019; Chu et al. 2019). Here we consider three objectives: classification error rate, multiply-adds and the number of parameters. We choose multiply-adds because we don't search models for specific hardware. We also impose a constraint on FLOPs to act as a requirement for mobile end. Moreover, we enforce an accuracy constraint to ensure minimal classification precision. It is not desired that a model with too many identity layers excels in FLOPs while behaving poorly in accuracy, also pointed out in (Chen et al. 2019). This constraint, however, indirectly regularizes the number of identity blocks in a model by barring out those with low performance.

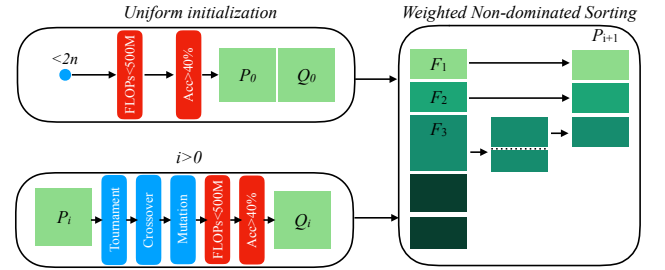


Figure 3: Constrained and weighted NSGA-II Pipeline.

To make fair comparisons, we make use of similar pipeline as FairNAS and only emphasize the differences if necessary. As Zhang et al. 2018 states, mobile models are prone to underfitting instead of overfitting. Therefore, we try to maximize the number of parameters, which can be informally regarded as a reward for high capacity. Classification accuracy and FLOPs are two critical objectives for practical applications. Taking all these aspects into account, we formulate our constrained weighted multi-objective problem as follows,

$$\begin{aligned} \min \quad & \{-Accuracy(m), FLOPs(m), -Params(m)\} \\ \text{s.t.} \quad & m \in \text{search space } S \\ & w_{acc} + w_{flops} + w_{params} = 1 \\ & w_{acc}, w_{flops}, w_{params} \geq 0. \\ & FLOPs(m) < FLOPs_{max}. \\ & Accuracy(m) > Acc_{min} \end{aligned} \quad (2)$$

Regarding a practical application, the weight of the above three objectives are chosen as $w_{acc} = 0.4$, $w_{flops} = 0.4$, $w_{params} = 0.2$. We also set $FLOPs = 500M$ and $Acc_{min} = 0.4$.

The control flow of our pipeline is shown in Figure 3. We use choice indices to encode the chromosome, for instance, $m_1 = (x_1^1, x_2^1, \dots, x_{19}^1)$.

Initialization We initialize population to introduce various choice blocks to encourage exploration.

Algorithm 1 The constrained and weighted NAS pipeline.

Input: Supernet S , the number of generations N , population size n , validation dataset D , constraints C , objective weights w

Output: A set of K individuals on the Pareto front.

Train supernet S defined on the scalable search space.

Uniformly generate the populations P_0 and Q_0 until each has n individuals satisfying C_{FLOPs} , C_{Accuracy} .

for $i = 0$ **to** $N - 1$ **do**

$R_i = P_i \cup Q_i$

$F = \text{non-dominated-sorting}(R_i)$

 Pick n individuals to form P_{i+1} by ranks and the crowding distance **weighted** by w .

$Q_{i+1} = \emptyset$

while $\text{size}(Q_{i+1}) < n$ **do**

$M = \text{tournament-selection}(P_{i+1})$

$q_{i+1} = \text{crossover}(M) \cup \text{mutation}(M)$ {Check the FLOPs constraint at first (It takes $< 1ms$).}

if $\text{FLOPs}(q_{i+1}) > \text{FLOPs}_{max}$ **then**

continue

end if

 Evaluate model q_{i+1} with S on D {Check the accuracy constraint (It takes $\approx 60s$).}

if $\text{Accuracy}(q_{i+1}) > \text{Acc}_{min}$ **then**

 Add q_{i+1} to Q_{i+1}

end if

end while

end for

Select K equispaced models near Pareto-front from P_N

Crossover Simply, we take single-point crossover.

Mutation We apply the same approach from FairNAS (Chu et al. 2019): a PPO based controller to encourage exploitation (Schulman et al. 2017) and a Roulette wheel selection to encourage exploration.

Weighted Non-dominated Sorting For practical uses, we weigh different preferences for various objectives by defining weighted crowding distance (Friedrich, Kroeger, and Neumann 2011). In particular, the weighted crowding distance $d = \sum_{i=0}^2 w_i d_i$ instead of $\sum_{i=0}^2 d_i$, where d_i is the crowding distance of the i th objective.

Ordered Constraints We organize these two hard constraints in order, because the costs for checking these two objectives vary significantly. In fact, while a model’s FLOPs can be obtained within 1 ms, its accuracy takes about 1 minute to evaluate. Therefore, we compute FLOPs first, those who violate the FLOPs constraint are eliminated thereon.

We run 120 epochs with a population size of 70 to get 8400 models. The search stage takes about 12 GPU days on a Tesla V100. Then we sample 3 models from the final Pareto front with approximately equal crowding distance and train them completely. The overall pipeline is detailed in Algorithm 1 and the hyperparameters for our pipeline is provided in the supplementary material.

Index	Expansion	Kernel Size	SE
0	3	3	-
1	3	3	✓
2	3	5	-
3	3	5	✓
4	3	7	-
5	3	7	✓
6	6	3	-
7	6	3	✓
8	6	5	-
9	6	5	✓
10	6	7	-
11	6	7	✓
12	-	1	-

Table 1: Each layer in our search space has 13 choices. Note index 12 is the identity block with LET.

Experiment Setup

Dataset

We perform the search directly on ImageNet 1k dataset (Deng et al. 2009) and randomly select 50k images from the training set as a validation set. The original validation set is used as the test set to report accuracy.

Search Space

We adopt a scalable MobileNetV2 search space with squeeze and excitation (SE) (Hu, Shen, and Sun 2018) to make fair comparisons with MnasNet (Tan et al. 2019) and EfficientNet (Tan and Le 2019).

Specifically, we utilize standard MobileNetV2 inverted bottleneck (Sandler et al. 2018) as building blocks after (Cai, Zhu, and Han 2019). We let the convolutional kernels be within $\{3, 5, 7\}$, expansion rates of $\{3, 6\}$, and an option of squeeze-and-excitation. The channel of filters per layer is retained. On top of this, we include an identity block with linearly equivalent transformation for scalability⁴. The overall size of search space arrives at 13^{19} . The detailed choice blocks per layer are displayed in Table 1. Note that Index 12 refers to an identity block with the equivalent transformation (1×1 Conv). The rest choices are typical MBV2 blocks.

Training Strategy

As for the training of the supernet, we follow the same settings as FairNAS, except that we train for 60 epochs. It takes about 10 GPU days.

For the full training stage, we also adopt the same configuration as Mnas (Tan et al. 2019) with standard Inception pre-processing tricks (Szegedy et al. 2017). Unlike EfficientNet, we don’t apply AutoAugment policy (Cubuk et al. 2018) because many state-of-the-art algorithms report their results without it. Moreover, we choose RMSProp optimizer with momentum 0.9. We use a batch size of 4096 and the initial learning rate of 0.256, which decays 0.01 every 2.4 epochs. The dropout rate is set to 0.2 (Srivastava et al. 2014)

⁴For downsampling, identity is replaced by a max pooling.

Models	Multi-Adds (M)	FLOPs Violation	Top-1 (%)	Top-5 (%)
All Identity	23	No	24.1	45.0
All K7E6	557	Yes	76.8	93.3

Table 2: Full train results of models with minimal and maximal FLOPs.

Methods	MAdds (M)	Params (M)	Top-1 (%)	Top-5 (%)
MobileNetV2 (2018)	300	3.4	72.0	91.0
MobileNetV3 (2019)	219	5.4	75.2	92.2
MnasNet -A1 (2019)	312	3.9	75.2	92.5
MnasNet-A2 (2019)	340	4.8	75.6	92.7
FBNet-B (2019)	295	4.5	74.1	-
Proxyless-R (2019)	320 [†]	4.0	74.6	92.2
Proxyless GPU (2019)	465 [†]	7.1	75.1	-
Single-Path (2019)	365	4.3	75.0	92.2
FairNAS-A (2019)	388	4.6	75.3	92.4
EfficientNet B0 (2019)	390	5.3	76.3	93.2
SCARLET-A (Ours)	365	6.7	76.9	93.4
SCARLET-B (Ours)	329	6.5	76.3	93.0
SCARLET-C (Ours)	280	6.0	75.6	92.6

Table 3: Comparison of neural models on ImageNet validation set. The input size is set to 224×224 . [†]: Based on its published code.

before the last FC layer and the weight decay ($l2$) rate to $1e - 5$.

Experiment Results

Evaluation of the Search Space

NAS results can benefit from good search spaces. To clarify the doubts that our method works without such design, also to alleviate the disturbance, we select two extreme models in view of FLOPs. The evaluation results are listed in Table 2. A model whose each layer is an identity block only scores 24.1% top-1 accuracy on ImageNet. Another extreme model obtains 76.8% at the cost of 557M FLOPs, which is an infeasible solution because of constraint violation. Therefore, it’s a challenging task to work on such search space for ordinary search techniques.

Comparison with State-of-the-art Methods

Table 3 gives a clear comparison of state-of-the-art models on ImageNet dataset. We pick models within the range of FLOPs from 200M to 400M. It is clear that our SCARLET series marks a new state of the art, with SCARLET-A surpassing EfficientNet-B0 with +0.5% increase on top-1 accuracy and 25M fewer FLOPs, SCARLET-B achieves the same top-1 accuracy with 61M fewer FLOPs. Although both A and B have higher numbers of parameters, this treatment should be encouraged as it is related to representational power and doesn’t necessarily increase inference latency. SCARLET-C also achieves a competing result with

+0.3% increase on top-1 accuracy compared with FairNAS-A, while costing 108M fewer FLOPs.

SCARLET-A makes full use of large kernels (five 5×5 and seven 7×7 kernels) to enlarge receptive field. Besides it activates many squeezing and excitation (12 out of 19) blocks to improve its classification performance. At the early stage, it appreciates either large kernels and small expansion ratios or small kernels and large expansion ratios to balance the trade-off between accuracy and FLOPs.

SCARLET-B chooses two identity operations. Compared with A, it shortens network depth at the last stages. Besides, it utilizes squeezing and excitation block extensively (14 out of 17). It places a large expansion block with large kernels at the tail stage.

SCARLET-C uses three identity operations and utilizes small expansion ratio extensively to cut down the FLOPs, large expansion ratio at the tail stage whose resolution is 7×7 . It prefers large kernels before the downsampling layers. Besides, it makes an extensive use of squeeze and excitation to boost accuracy.

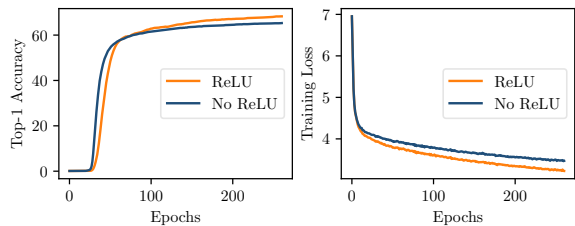


Figure 4: Training of a random model where identity blocks are enabled with linear transformation (No ReLU) vs. with non-linear transformation (ReLU).

Scaling up Models

We scale our models up to evaluate their performance for higher accuracies. Noticing the high cost of EfficientNet (Tan and Le 2019), where grid search is utilized for a good configuration for input resolution, channel and depth multiplier, we simply artificially scale our models. In particular, we use the same input dimension as EfficientNet, and adjust the channel multiplier to reach comparable FLOPs as their counterparts EfficientNet-B2 and B4. Most previous methods don’t use fixed AutoAugment trick (Cubuk et al. 2018), we abstain from it too. We follow the rest training settings as (Tan and Le 2019). Besides, we use a dropout of 0.3 for SCARLET-A2 and 0.4 for A4. The performance of scaled models are listed in Table 4. We obtain superior accuracies although we don’t perform grid search or the fixed AutoAugment trick. Remarkably, fixed data augmentation improves performance especially for larger models, which can further boost the performance of our upscaled models.

Ablation Study

Equivalent Transformation vs. Identity To check the validity of our method, we utilize identity as a basic choice to act as the baseline group, which is commonly used in prior works. We train the two supernet under the same training

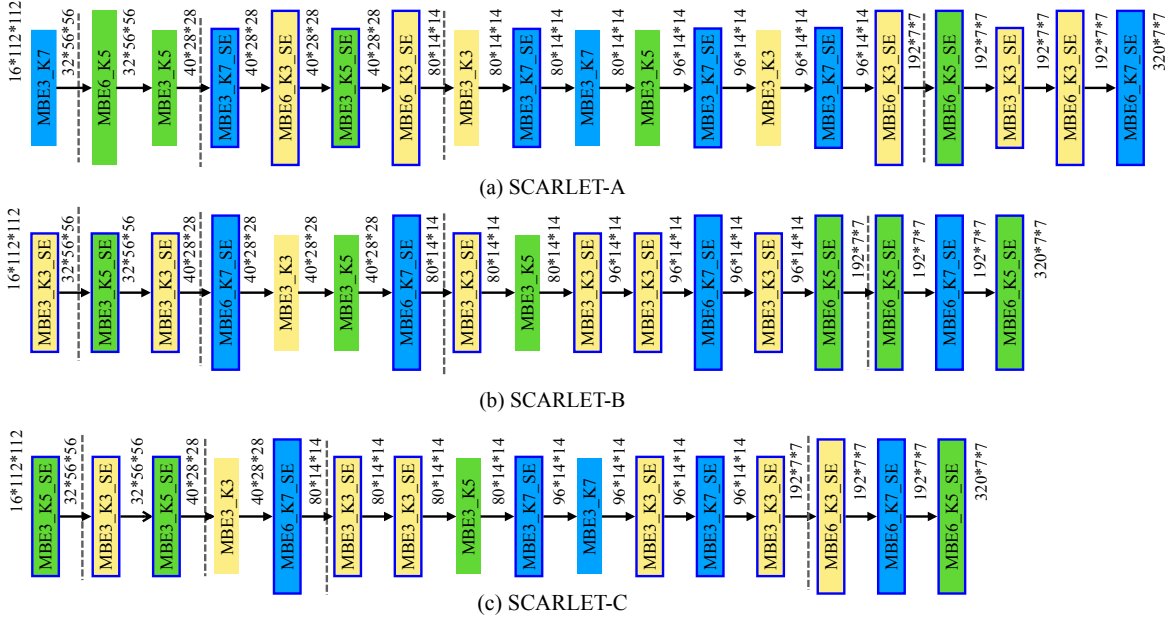


Figure 5: The architectures of SCARLET-A,B,C. Notice the dashed lines refer to downsampling points. The stem and tail parts are omitted. Best viewed in color.

Methods	Resolution	Depth (\times)	Channel (\times)	MAdds (B)	Params (M)	Top-1 (%)	Top-5 (%)
DenseNet-264 (2017)	224 \times 224	-	-	6	34	77.9	93.9
Xception (2017)	299 \times 299	-	-	8.4	23	79.0	94.5
EfficientNet B2 (2019)	260 \times 260	1.2	1.1	1.0	9.2	79.4* (79.8)	94.7* (94.9)
SCARLET-A2 (ours w/o fixed AutoAugment)	260 \times 260	1.0	1.4	1.0	12.5	79.5	94.8
ResNeXt-101 (2017)	320 \times 320	-	-	32	84	80.9	95.6
PolyNet (2017)	331 \times 331	-	-	35	92	81.3	95.8
EfficientNet B4 (2019)	380 \times 380	1.8	1.4	4.2	19	81.9* (82.6)	95.8* (96.3)
SCARLET-A4 (ours w/o fixed AutoAugment)	380 \times 380	2.0	1.4	4.2	27.8	82.3	96.0

Table 4: Single-crop results of scaled architectures on ImageNet validation set. *: Retrained w/o fixed AutoAugment. Those within parentheses are w/ fixed AutoAugment, reported by its authors.

setting for 60 epochs. We report the average training accuracy and standard variance per epoch in Figure 1. Our method with linearly equivalent transformation can obtain about 20% higher than the baseline in case of the top-1 accuracy on the training set. Moreover, it exhibits much lower variance, which indicates each model is trained more fairly. Further, we sample all the models in the last epoch and report their metrics by a histogram, which is shown at the bottom part of Figure 1. Identity makes troubles for the training and quite some models suffer seriously and their metrics are below 30%. Therefore, they are severely underestimated by the supernet, whereas LET can compensate and bring the models to a reasonable range.

Equivalent vs Non-equivalent Transformation Here we show that non-equivalent transformation changes the representative power of neural networks. A simple modification by adding ReLU function can violate the equivalence.

To prove this, we randomly sample a model meta and then forcibly flip some choice blocks to identity : (1, 3, 1, 0, 12, 0, 0, 0, 12, 12, 12, 12, 12, 0, 0, 0, 12, 12, 9). We train this model with ReLU (non-equivalent) and without (equivalent) for identity layer. on the same seeds, training tricks, initialization strategy, and hyperparameters. Figure 4 indicates that a trivial modification non-negligibly affects its representative power. While in our scalable supernet, we have to guarantee an equivalent transformation and this is why ReLU can't apply.

Identity Regularization Our NAS approach is formulated as a constrained MOP. On the one hand, according to the dominance definition in NSGA-II, a model composed by all identity operations possesses minimal FLOPs, which are not dominated by any other individuals (standing on rank 0). On the other hand, it is also a boundary node as per FLOPs, which is never removed because of infinite crowding dis-

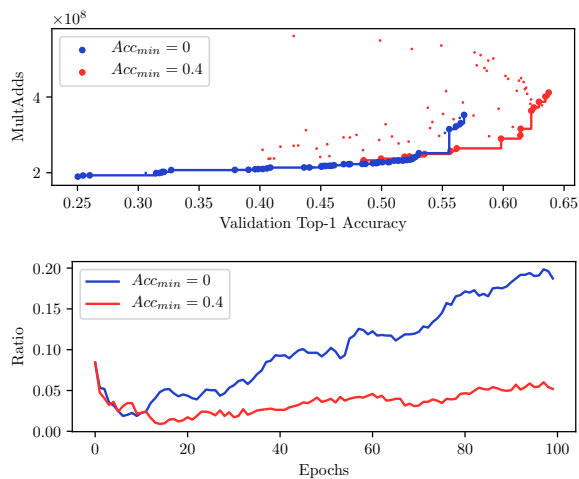


Figure 6: Ablation study on constrained optimization. **Top:** Pareto front of MultAdds vs. Accuracy. **Bottom:** The ratios of identity blocks per epoch.

tance (Deb et al. 2002). In this way, too many harmful genes contaminates the population pool. To verify this, we design two experimental groups: $Acc_{min} = 0.4$ (with a minimum accuracy constraint) and $Acc_{min} = 0.0$ (without such a constraint).

We use the same trained supernet as the model accuracy predictor and apply the same hyperparameters for the NAS pipeline to search for the best models. We run 100 epochs with a population size of 70. We plot the Pareto front for the last generation P_{100} in the top of Figure 6. We observe that, without the constraint, the generated models locate within a range (0.25, 0.57). Whereas $Acc_{min} = 0.4$, the models shift to a better range (0.4, 0.65). We also compute statistics about the identity operation ratio within P along with the evolution process, which is shown at the bottom of Figure 6. The ratio is initially about 0.08 ($\approx \frac{1}{13}$) for both cases. The former one enlarges this ratio continually and reaches about 0.2 in the end, in contrast, the latter regularizes this ratio to a stable value around 0.05, which confirms our prior analysis. Therefore, this accuracy constraint for practical purposes can be considered as regularization for identity.

Discussion and Future Work

Weight sharing is one of the most critical features for efficient neural architecture search. Most of the one-shot approaches concentrate on how to find useful networks from choosing parallel choices. This schema hardly meets the requirement for flexibility, it even causes conflicts inherently. Since a neural network learns features layer by layer, it's highly sensitive to any scaling operation. Our equivalent transformation can be regarded as a buffer for such operations. Nevertheless, it works best under some conditions. In our search spaces, a linear transformation is used to match a single inverted bottleneck layer, where only two non-linear activation functions are involved. When the matched function is too complicated, it will be more difficult to compen-

sate.

How to perform flexible search efficiently remains open. Google's reinforced approach on top of huge computing resource (Zoph et al. 2018; Tan et al. 2019) is neither affordable nor environmental friendly. One of our future works is making the search process both flexible and efficient.

Related Works

One-Shot Neural Architecture Search

In one-shot approaches, a supernet is constructed to represent the whole search space, within which each path is a stand-alone model. The supernet is trained only once, child models can inherit the weights of supernet thus it is easier and faster to evaluate its performance compared with other incomplete training techniques. Notable works are (Bender et al. 2018; Stamoulis et al. 2019; Guo et al. 2019; Cai, Zhu, and Han 2019). Recent advances are concerned with ranking ability in the search phase (Sciuto et al. 2019). FairNAS improves ranking efficiency by enforcing a strict fairness constraint. Nevertheless, the scalability of a supernet is not well investigated in these methods, which restricts its flexibility to discover potent candidate architectures.

Scalability and Network Transformation

Given a neural network, it has been experimentally studied to scale its size up or down for various application scenarios. Common model upscaling practices include increasing depth, width, as well as input image resolution (He et al. 2016; Zagoruyko and Komodakis 2016; Huang et al. 2018). Recent work by (Tan and Le 2019) proposes an effective compound scaling method that incorporates all three with a balance achieved by grid search. Nevertheless, these methods leave parameter sharing out of the discussion, each scaled network has to be trained from scratch. Network transformation is a solution for model scaling by reusing the weights from the original structure. For instance, Net2Net by (Chen, Goodfellow, and Shlens 2015) invented two transformation schemes to pass on parameters to either wider or deeper student networks.

Conclusion

In this paper, we unveil the overlooked scalability issue in one-shot neural architecture search approaches. We show that simply adding identity blocks introduces training instability. By compensating the learning process with linearly equivalent transformation, we fill the gap between scalability and stability. We prove and demonstrate such transformation is identical in terms of representational power. The renewed supernet then can be trained with desired convergence and delivers competitive neural architectures. Namely, with fewer FLOPs than EfficientNet-B0, SCARLET-A achieves 76.9% Top-1 accuracy on ImageNet. SCARLET-B illustrates that shallow models can perform better which hits the same 76.3% as EfficientNet-B0 with much reduced FLOPs. SCARLET-C strikes 75.6%, also exceeds its peers of similar sizes. Upscaled SCARLET-A2 and A4 are comparable to EfficientNet-B2, B4 separately too.

References

- Bender, G.; Kindermans, P.-J.; Zoph, B.; Vasudevan, V.; and Le, Q. 2018. Understanding and Simplifying One-Shot Architecture Search. In *International Conference on Machine Learning*, 549–558.
- Brock, A.; Lim, T.; Ritchie, J. M.; and Weston, N. 2018. SMASH: One-Shot Model Architecture Search Through HyperNetworks. *International Conference on Learning Representations*.
- Cai, H.; Zhu, L.; and Han, S. 2019. ProxylessNAS: Direct Neural Architecture Search on Target Task and Hardware. In *International Conference on Learning Representations*.
- Chen, X.; Xie, L.; Wu, J.; and Tian, Q. 2019. Progressive Differentiable Architecture Search: Bridging the Depth Gap between Search and Evaluation. *arXiv preprint. arXiv:1904.12760*.
- Chen, T.; Goodfellow, I.; and Shlens, J. 2015. Net2Net: Accelerating Learning via Knowledge Transfer. In *International Conference on Learning Representations*.
- Chollet, F. 2017. Xception: Deep Learning with Depthwise Separable Convolutions. In *Proceedings of the IEEE Conference on Computer Vision and Pattern Recognition*, 1251–1258.
- Chu, X.; Zhang, B.; Xu, R.; and Li, J. 2019. FairNAS: Rethinking Evaluation Fairness of Weight Sharing Neural Architecture Search. *arXiv preprint. arXiv:1907.01845*.
- Cubuk, E. D.; Zoph, B.; Mane, D.; Vasudevan, V.; and Le, Q. V. 2018. AutoAugment: Learning Augmentation Policies from Data. *arXiv preprint. arXiv:1805.09501*.
- Deb, K.; Pratap, A.; Agarwal, S.; and Meyerivan, T. 2002. A Fast and Elitist Multiobjective Genetic Algorithm: NSGA-II. *IEEE Transactions on Evolutionary Computation* 6(2):182–197.
- Deng, J.; Dong, W.; Socher, R.; Li, L.-J.; Li, K.; and Fei-Fei, L. 2009. ImageNet: A Large-Scale Hierarchical Image Database. In *Proceedings of the IEEE Conference on Computer Vision and Pattern Recognition*, 248–255. IEEE.
- Friedrich, T.; Kroeger, T.; and Neumann, F. 2011. Weighted Preferences in Evolutionary Multi-Objective Optimization. In *Australasian Joint Conference on Artificial Intelligence*, 291–300. Springer.
- Guo, Z.; Zhang, X.; Mu, H.; Heng, W.; Liu, Z.; Wei, Y.; and Sun, J. 2019. Single Path One-Shot Neural Architecture Search with Uniform Sampling. *arXiv preprint. arXiv:1904.00420*.
- He, K.; Zhang, X.; Ren, S.; and Sun, J. 2016. Deep Residual Learning for Image Recognition. In *Proceedings of the IEEE Conference on Computer Vision and Pattern Recognition*, 770–778.
- Howard, A.; Sandler, M.; Chu, G.; Chen, L.-C.; Chen, B.; Tan, M.; Wang, W.; Zhu, Y.; Pang, R.; Vasudevan, V.; et al. 2019. Searching for MobileNetV3. *arXiv preprint. arXiv:1905.02244*.
- Hu, J.; Shen, L.; and Sun, G. 2018. Squeeze-and-Excitation Networks. In *Proceedings of the IEEE Conference on Computer Vision and Pattern Recognition*, 7132–7141.
- Huang, G.; Liu, Z.; Van Der Maaten, L.; and Weinberger, K. Q. 2017. Densely Connected Convolutional Networks. In *Proceedings of the IEEE Conference on Computer Vision and Pattern Recognition*, 4700–4708.
- Huang, Y.; Cheng, Y.; Chen, D.; Lee, H.; Ngiam, J.; Le, Q. V.; and Chen, Z. 2018. GPipe: Efficient Training of Giant Neural Networks using Pipeline Parallelism. *arXiv preprint. arXiv:1811.06965*.
- Lu, Z.; Whalen, I.; Boddeti, V.; Dhebar, Y.; Deb, K.; Goodman, E.; and Banzhaf, W. 2019. NSGA-NET: A Multi-objective Genetic Algorithm for Neural Architecture Search. In *The Genetic and Evolutionary Computation Conference*.
- Sandler, M.; Howard, A.; Zhu, M.; Zhmoginov, A.; and Chen, L.-C. 2018. MobileNetV2: Inverted Residuals and Linear Bottlenecks. In *Proceedings of the IEEE Conference on Computer Vision and Pattern Recognition*, 4510–4520.
- Schulman, J.; Wolski, F.; Dhariwal, P.; Radford, A.; and Klimov, O. 2017. Proximal Policy Optimization Algorithms. *arXiv preprint. arXiv:1707.06347*.
- Sciuto, C.; Yu, K.; Jaggi, M.; Musat, C.; and Salzmann, M. 2019. Evaluating the Search Phase of Neural Architecture Search. *arXiv preprint. arXiv:1902.08142*.
- Srivastava, N.; Hinton, G.; Krizhevsky, A.; Sutskever, I.; and Salakhutdinov, R. 2014. Dropout: A Simple Way to Prevent Neural Networks from Overfitting. *The Journal of Machine Learning Research* 15(1):1929–1958.
- Stamoulis, D.; Ding, R.; Wang, D.; Lymberopoulos, D.; Priyanka, B.; Liu, J.; and Marculescu, D. 2019. Single-Path NAS: Designing Hardware-Efficient ConvNets in less than 4 Hours. *arXiv preprint. arXiv:1904.02877*.
- Szegedy, C.; Ioffe, S.; Vanhoucke, V.; and Alemi, A. A. 2017. Inception-v4, Inception-ResNet and the Impact of Residual Connections on Learning. In *Thirty-First AAAI Conference on Artificial Intelligence*.
- Tan, M., and Le, Q. V. 2019. EfficientNet: Rethinking Model Scaling for Convolutional Neural Networks. In *International Conference on Machine Learning*.
- Tan, M.; Chen, B.; Pang, R.; Vasudevan, V.; and Le, Q. V. 2019. Mnasnet: Platform-Aware Neural Architecture Search for Mobile. In *Proceedings of the IEEE Conference on Computer Vision and Pattern Recognition*.
- Wu, B.; Dai, X.; Zhang, P.; Wang, Y.; Sun, F.; Wu, Y.; Tian, Y.; Vajda, P.; Jia, Y.; and Keutzer, K. 2019. FBNet: Hardware-Aware Efficient ConvNet Design via Differentiable Neural Architecture Search. *The IEEE Conference on Computer Vision and Pattern Recognition*.
- Xie, S.; Girshick, R.; Dollár, P.; Tu, Z.; and He, K. 2017. Aggregated Residual Transformations for Deep Neural Networks. In *Proceedings of the IEEE Conference on Computer Vision and Pattern Recognition*, 1492–1500.
- Zagoruyko, S., and Komodakis, N. 2016. Wide Residual Networks. In *Proceedings of the British Machine Vision Conference*.
- Zhang, X.; Li, Z.; Change Loy, C.; and Lin, D. 2017. PolyNet: A Pursuit of Structural Diversity in Very Deep Networks. In *Proceedings of the IEEE Conference on Computer Vision and Pattern Recognition*, 718–726.
- Zhang, X.; Zhou, X.; Lin, M.; and Sun, J. 2018. ShuffleNet: An Extremely Efficient Convolutional Neural Network for Mobile Devices. In *The IEEE Conference on Computer Vision and Pattern Recognition*.
- Zoph, B.; Vasudevan, V.; Shlens, J.; and Le, Q. V. 2018. Learning Transferable Architectures for Scalable Image Recognition. In *Proceedings of the IEEE Conference on Computer Vision and Pattern Recognition*, 8697–8710.